Geotech Geol Eng (2024) 42:2845–2859
https://doi.org/10.1007/s10706-023-02709-w

ORIGINAL PAPER

Uplift Performance of Suction Foundations in Sandy Soils for Offshore Platforms

Wenbin Xu · Ke Wu · Haotian Luo · Zhenhua Liu · Zhongyu Dou · Dongxue Hao

Received: 17 July 2023 / Accepted: 28 November 2023 / Published online: 26 December 2023

Abstract Suction foundations are widely used in the construction of offshore platforms. Their uplift resistance in sandy soil strata is crucial for evaluating the stability of offshore platforms. A scaled-down experimental device was developed to investigate the pull-out performance of suction-type foundations in sandy soil. The relationship between the pull-out performance of suction-type foundations under the influence of different factors (e.g. different uplift directions) and the uplift speed was discussed. The ABAQUS finite element explicit dynamic analysis method was used to study the influence of different drainage conditions, loading speeds, loading angles, and loading methods on the stress change, deformation, and bearing performance of the surrounding soil during the design stage of the suction foundation. The comprehensive testing and numerical analysis results revealed the pull-out performance of suction foundations in sandy soils. The results showed that the uplift performance of the suction foundation is affected by the uplift angle and speed. At low uplift angles, increasing the uplift speed can improve the ultimate bearing capacity of the suction foundation, while at high uplift angles, a lower uplift speed can help improve its uplift resistance. At the same time, the ultimate bearing capacity of the complete drainage simulation is generally higher, which can provide a more conservative safety estimate for engineering design.

Keywords Suction caisson · Pull-out performance · Test · Numerical calculation

1 Introduction

The marine industry is one of China's strategic emerging industries and one of the important sectors that promote sustainable economic development and ensure national energy security. In a marine environment, the corrosion caused by seawater, wave impact, and other factors have resulted in foundations that are easily affected by the uplift force; hence, floating marine structures require foundations that provide continuous and stable uplift resistance. The requirements for the pull-out resistance of foundations are very high. As a relatively stable basic structure, the suction foundation must have a strong pull-out resistance to withstand the pull-up forces from various angles and directions; effectively resist the impact of the marine environment, such as waves and wind; and minimise the risk of the structure overturning. In the marine sandy soil stratum, the pull-out performance

W. Xu · K. Wu (✉) · H. Luo · Z. Liu · Z. Dou
School of Civil Engineering, Shandong University, Jinan 250061, Shandong, China
e-mail: wk4223@163.com

D. Hao
School of Civil Engineering and Architecture, Northeast Electric Power University, Jilin 132012, Jilin, China

of the suction foundation is significantly affected by the unique properties of the sandy soil.

Numerous scholars have conducted extensive research (i.e. experiments, theoretical analyses, and numerical calculations) on this topic. Acosta-Martinez et al. (2008), Cao (2003), Du et al. (2017), Chen et al. (2012), Lehane et al. (2008), and Purawana et al. (2005) showed that the bottom reaction of foundations could improve its uplift bearing capacity and that the reaction force could be used as a part of the pull-out capacity. Kim et al. (2015) investigated the pullout performance of multiple suction-bucket foundations in silty sand under horizontal loads through centrifuge model tests and numerical simulations. They found that the average uplift force of the entire anchoring system increased with the increasing load angle. The numerical simulations were also validated against the experimental results. Bang et al. (2011) conducted a series of centrifuge model tests to study the inclined pullout bearing capacity of suction-bucket models embedded in sandy soil. They compared the analytical solution for oblique ultimate bearing capacity under eccentric vertical loading conditions with experimental results and discussed the performance differences related to load inclination angles and mooring points. They established an analytical solution for the horizontal pullout load capacity utilizing three-dimensional soil failure. Ssenyondo (2021) employed a large-scale model test system to study the influence of different burial depths on the uplift capacity of bucket foundations in sandy soil, with burial depth ranging from 0.5 times to 2 times the bucket diameter. The results showed that the uplift capacity increased with increasing burial depth, reaching a peak at the optimal burial depth, and then decreased with further increases in burial depth. Vicent (2020) conducted vertical uplift tests on bucket foundations in sandy soil under varying loading rates using a 1 g model test system. The results indicated that loading rate significantly affects the uplift capacity of bucket foundations, with different growth trends observed as the loading rate increased. Fatolahzadeh (2020) investigated the influence of rock substrates on the behavior of square shallow foundations. By conducting small-scale laboratory experiments, variations in skirt length and rock depth were explored, subjecting sandy soils of different densities to vertical loading, and examining the impact of rock presence on the foundation. Xu et al. (2023) investigated the tensile load-bearing capacity of suction caissons in the design of offshore wind turbine foundations and introduced a computational method that accounts for soil stress release and differential pressure contribution. The research results demonstrate that differential pressure significantly affects the tensile capacity of suction caissons under different drainage conditions, with distinct design disparities between fully drained and undrained scenarios. Rasmussen et al. (1991), Christensen et al. (1991), Renziet et al. (1991), Steensen-Bach et al. (1992), Cluckey et al. (2004), Dyvik et al. (1993), Morrison et al. (1994), Deng et al. (2002) Rahman et al. (2001), and Allersma et al. (2003) conducted theoretical analyses on the vertical limit uplift bearing capacity of suction bucket foundations. They performed a full theoretical derivation, taking into account the influence of factors such as the base length-to-diameter ratio, soil properties, and uplift speed. Qiu (2017), based on the limit equilibrium theory, derived a calculation formula for the ultimate uplift capacity of caisson foundations, considering the impact of soil strength anisotropy and caisson foundation stiffness. Dai (2019), employing the limit analysis method, derived an upper bound solution to determine the ultimate uplift load capacity of suction foundations in sandy soil. The analysis involved the utilization of Prandtl and Hill's reverse failure mechanisms in calculating the uplift capacity of suction caisson foundations. Samui et al. (2011) proposed a calculation formula for the pullout bearing capacity of suction-bucket foundations in clay based on a multivariate adaptive regression spline method. The formula considered the uplift velocity coefficient, foundation aspect ratio, loading angle, and undrained shear strength of the soil. By comparing the calculation results with finite element analysis, the applicability of the multivariate adaptive regression spline method in estimating pullout bearing capacity was verified. Zhao et al. (2016) introduced a numerical simulation method that incorporates the anchor chain effect into a coupled Euler–Lagrange analysis to study comprehensive anchoring behavior. This method was demonstrated to provide a more accurate simulation of the response of the anchoring system, considering the interaction between the anchor chain and the soil. Liu et al. (2014) conducted a comparative numerical simulation study on the failure modes of traditional suction-bucket foundations and wide-shallow suction-bucket foundations. They proposed

new simplified calculation methods for vertical load capacity and overturning stability. Overturning stability was determined using a safety factor method and depended on the location of the pivot point. Senders (2008) focused on predicting the environmental load conditions of typical tripod suction-bucket foundations in dense sandy soil using numerical simulations. Centrifuge model tests were conducted to validate the prediction results of the calculation program. The study results indicated that suction-bucket foundations exhibit weaker pullout performance in sandy soil but have higher pullout resistance under compressive loads. Shen et al. (2022) investigated the influence of partial drainage on the pullout behavior of suction bucket foundations in saturated sandy soil, employing a coupled hydraulic-mechanical finite element model that considered seepage and pore water pressure dissipation during the installation and pullout processes. Fattahi and Zandy Ilghani(2023) successfully estimated the behavior of suction caissons in clay by employing Monte Carlo Markov Chain (MCMC) and GMDH neural network models. They used parameters such as Teta (inclined angle), L/d (embedded length-to-diameter ratio), Tk (load rate parameter), Su (undrained shear strength of soil), and D/L (depth ratio) as inputs to effectively predict the pullout capability of suction caissons. Patel and Singh (2019) utilized a three-dimensional finite element method to study the vertical uplift capacity of suction caisson foundations in cohesive soil, exploring various parameters such as caisson diameter, skirt length, undrained shear strength of the soil, and installation depth on the uplift capacity. In conclusion, scholars have conducted in-depth research on the uplift performance of suction foundations in sandy soil layers for offshore oil platforms. This research not only provides essential theoretical support for the safety and stability of marine platforms but also serves as a reference for the further improvement and optimization of suction foundations.

The numerical simulation static analysis of Duyu bucket foundation in the current research has been relatively perfect. Considering the loads such as wind and waves are not simple and slow loading, if only the static bearing capacity analysis is used, there will be a big gap with the actual working conditions. In this study, an experimental device was developed to investigate the pull-out performance of a suction-type foundation in sandy soil. Scaled-down tests were conducted to examine the influence of factors such as different uplift directions and speeds and the failure mode. The ABAQUS finite element display dynamic analysis method was used to examine the effects of various drainage conditions, loading speeds, loading angles, and loading methods on the surrounding soil stress change, deformation, and bearing performance during the design stage of the suction foundation. A comprehensive test based on the numerical research results demonstrated the pull-out performance of suction foundations in sandy soils, which can provide a more conservative safety estimate for engineering design.

2 Experimental Research

Scaled-down tests, which reduce the scale of an actual engineering structure, are widely used in laboratory conditions. The experiment in this study adopted a precise scaled-down test method to ensure the reliability and practicability of the results. The experiment first focused on the bearing performance of the suction foundation under displacement-velocity control. Then, the uplift behaviour of the suction foundation under dynamic loading conditions was studied until its bearing capacity failed. During the experiment, different loading rates and drainage conditions were considered to study the effects of the degree of pore-water pressure dissipation in the foundation soil and the failure mode of the vertical uplift of the suction foundation. The experimental results are poised to elucidate that three failure modes in the suction foundation (local shear failure, bottom tension failure, and overall failure) could occur in the three potential scenarios of complete drainage, partial drainage, and complete non-drainage.

2.1 Test Model and Test Device

2.1.1 Test Model

The suction barrel-shaped foundation model used in this test is a 304 stainless steel customized scale model. The specific parameters are as follows: a diameter of 102 mm, length of 100 mm (length-to-diameter ratio $\approx$ 1), and wall thickness of 3 mm, as shown in Fig. 1. To facilitate the experimental process and data collection, a vertical nut was welded

Fig. 1 Bucket foundation scale model

to the centre of the top of the model. During the experiment, the nuts were connected to steel strands to facilitate the application of a pulling force to the barrel foundation. A 3 mm hole was drilled at the top of the barrel-shaped foundation to keep the pressure inside and outside the barrel consistent during installation. This allows the barrel-shaped foundation to sink quickly and minimises the disturbance of the surrounding sand.

2.1.2 Test Device

The self-developed testing device in Fig. 2 can conduct pull-up tests on the barrel-shaped foundation model at different angles and speeds. By collecting time-displacement data, the displacement load uplift capacity curve of the suction bucket foundation was obtained, and the uplift bearing performance of the suction bucket foundation was studied. The device consists of the following parts: precision sliding table set, load sensor, pulley, movable plate group, steel strands, and sand container. The sliding table and pulley were fixed on the movable plate, and the preset displacement and speed were applied through the steel strand. The movable plate could be moved up and down and fixed to change the uplift angle of the barrel foundation. The pulleys converted different pull-up angles into vertical pulls. The sand container was located above the bottom of the movable plate group and used to fix the entire experimental device. The container is made of PVC material and has good corrosion and wear resistance. Its length, width, and height are 700 mm, while its wall thickness is 10 mm to maintain its stability and structural integrity when subjected to the short-term vibrations of the shaking table. The suction caisson foundation model, with a diameter of 102 mm, is typically considered to be "significantly smaller than" the dimensions of the containment vessel. Consequently, there exists ample space between the model and the vessel walls to simulate infinite boundary conditions. Additionally, the employment of precision instrumentation and the superior mass of the vibration table collectively serves to ameliorate the influence of boundary effects. The suction caisson foundation model, with a diameter of 102 mm, is typically considered to be "significantly smaller than" the dimensions of the containment vessel. Consequently, there exists ample space between the model and the vessel walls to simulate infinite boundary conditions. Additionally, the employment of precision instrumentation and the superior mass of the vibration table collectively

Fig. 2 The experimental device

serves to ameliorate the influence of boundary effects. The precision slide set consisted of a precision slide, CL-01A controller, LRS-100-24 power supply, and DM20 driver. It can be programmed to apply a displacement load and return to its initial position to ensure the integrity of the experimental process. The load sensor monitors the load applied to the barrel foundation model in real time, converts the load signal to an electrical signal, and records the load data in real time. These data can be used to analyse the uplift performance of barrel foundations under different working conditions (Fig. 3).

2.2 Test Method

2.2.1 Sand Sample Preparation

Due to the susceptibility of sand to disturbance, obtaining undisturbed sand samples in laboratory geotechnical testing is challenging. Different sampling processes and methods have a significant impact on the mechanical properties of sand. The vibration method is an important technique in geotechnical testing for preparing saturated sand samples, as described in reference (Vaid et al. 1988). This method achieves compaction through vibration to achieve a dense state. The saturated sand samples were prepared in the PVC sand container on the vibrating table. First, the container was filled with standard sand layer-by-layer; each layer has a thickness of approximately 50–100 mm. After each layer of sand was added, it must be levelled to ensure its even distribution. Then, the appropriate amount of water was added to fully saturate it. Artificial spraying was used to add water to prevent sand particles from floating. After water was added to each layer of sand, the container was vibrated on the vibrating table. The vibration time and frequency were adjusted according to the test requirements and specific equipment. The vibration process rearranged the sand particles, which improved compaction. The above steps were repeated until the container was full and the required sand height was reached.

2.2.2 Test Plan

A series of tests (6×4 tests) were conducted on the saturated standard sand. The details are listed in Table 1. According to different loading speeds and loading angles, the angle between the uplift and horizontal directions was used as the loading angle. Six different loading angles (0°, 15°, 30°, 45°, 60°, and 75°) and four different loading speeds (0.3, 0.5, 1, and 2 mm/s) were applied. These test parameters cover the uplift performance of suction bucket foundations under various conditions.

Velocity-displacement controlled loading was adopted for the test. To accurately explore the pull-out performance of the suction bucket foundation under different conditions, the controller was programmed

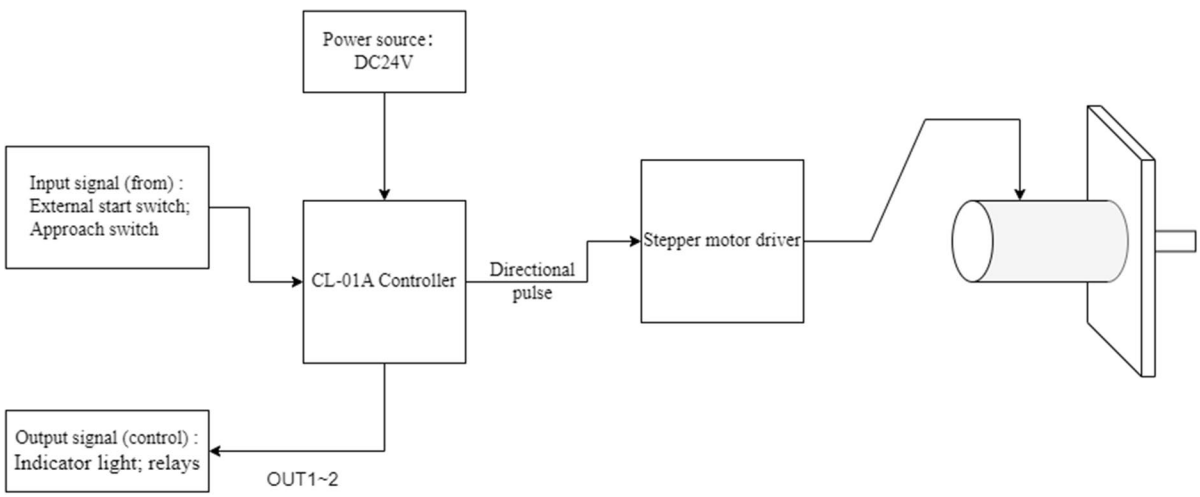

Fig. 3 Schematic diagram of controller connection

Table 1 Pull-up uniform loading test program

Test No	Loading angle (°)	Loading speed (mm/s)	Number of trials
P-75–03	75	0.3	2
P-75–05	75	0.5	2
P-75–10	75	1	2
P-75–20	75	2	2
P-60–03	60	0.3	2
P-60–05	60	0.5	2
P-60–10	60	1	2
P-60–20	60	2	2
P-45–03	45	0.3	2
P-45–05	45	0.5	2
P-45–10	45	1	2
P-45–20	45	2	2
P-30–03	30	0.3	2
P-30–05	30	0.5	2
P-30–10	30	1	2
P-30–20	30	2	2
P-15–03	15	0.3	2
P-15–05	15	0.5	2
P-15–10	15	1	2
P-15–20	15	2	2
P-00–03	0	0.3	2
P-00–05	0	0.5	2
P-00–10	0	1	2
P-00–20	0	2	2

to set the loading mode to uniform loading during the experiment. Each group of experiments was repeated twice to ensure the reliability of the data. The reliability of the test was verified by comparison. If the difference between the results of two tests and the maximum fluctuation exceeded 5%, a third test was conducted to eliminate testing errors. During the test, the load-time data collected by the load sensor was monitored in real time to adjust the test parameters and control the devices. The load–displacement curve was obtained by processing the load-time data. The ultimate bearing capacity of the suction bucket foundation was determined according to the curve characteristics.

2.3 Results and Discussion

1. Analysis of the influence of the uplift angle on the uplift performance of the suction foundation

In the 6×4 sets of indoor tests, four sets of tests were conducted on the displacement loading at six different loading angles and speeds. According to the test results, the influence of different loading angles on the failure mode of the suction foundation were analysed.

Figure 4 shows the effects of different uplift angles on the failure mode of the suction foundation. (1) Under low-angle loading, the failure mode was mainly horizontal loading failure, and the suction foundation model was dominated by horizontal displacement. The suction foundation exhibited an obvious overturning as a whole. The performance of the bearing capacity was compared with that of the large model. The uplift angle was stronger. After drainage treatment, it was found that the sand in the bucket did not separate from the lower soil as a whole. Complete drainage was the main process during uplift. The friction and earth pressure between the barrel and soil provided the pull-out capacity. (2) At a loading angle of over 30°, the barrel foundation had two failure modes. (1) At a lower loading speed, the barrel body at a low angle showed an obvious uplift process. After drainage, it was found that the sand in the barrel did not separate from the lower soil as a whole. The sandy soil facing away from the displacement direction of the barrel had a small deformation and retained its original shape, while the top of the soil facing the displacement direction of the barrel had obvious circular deformation. (2) When the suction foundation was uplifted at a high angle, partial drainage and non-drainage failure modes appeared, and the foundation moved upward along with its internal soil. Owing to the low loading speed of the entire test and continuous uplifting process, the negative pressure in the foundation gradually decreased, and the effect of soil plugging decreased.

Figure 5 shows the effects of different uplift angles on the ultimate bearing capacity of the suction foundation. At the same uplift speed, the uplift angle increased as the ultimate bearing capacity of the suction foundation gradually decreased. This indicates that the uplift angle has a certain influence on the uplif performance of the suction foundation.

2. Analysis of the influence of uplift speed on the uplift performance of suction foundation

(a) 15° pull-up drawing of bucket foundation (b) 45° pull-up drawing of bucket foundation

Fig. 4 Pull-up drawing of the bucket foundation under different uplift angles

As shown in Fig. 5, the uplift speed at different angles had different effects on the uplift performance of the suction foundation. At smaller uplift angles, the effect of the uplift speed on the uplift performance was more evident. At larger uplift angles, the effect of the uplift speed on the uplift performance was relatively small. This indicates that in practical engineering applications, the uplift speed can be adjusted according to the actual situation to optimise the uplift performance of the barrel foundation. Figure 6 shows the ultimate bearing capacity of the suction foundation at different uplift speeds. (1) At a low loading speed of 0.3 mm/s, the ultimate bearing capacity of the suction foundation formed a relatively smooth envelope, which indicates the relative stability of the pull-out performance of the suction foundation. (2) At a low angle, the ultimate bearing performance of the suction foundation clearly improved as the uplift speed increased This may be related to the influence of the uplift speed on the friction resistance between the sand and foundation at a small uplift angle. (3) At uplift angles of 30°, 45°, and 60°, the variations in the ultimate bearing capacity of the suction foundation was relatively small, which indicates the weak influence of the uplift speed on the uplift performance. (4) At the uplift angle of 75°, the increase in the uplift velocity resulted in partial drainage, which could decrease the frictional resistance of the sand to the foundation. (5) At the same uplift angle, the ultimate bearing capacity of the suction foundation gradually increased as the uplift velocity increased. This indicates that a higher uplift velocity improved the uplift performance of the suction foundation.

3 Numerical Calculation and Analysis

3.1 Numerical Calculation Model

The scaled-model test was presented in the ABAQUS finite element program to study the pull-out performance of the suction foundation. The diameter of the suction foundation model is D = 102 mm, the barrel height is H = 100 mm (H/D≈1), and the wall thickness is 3 mm. To ensure the accuracy of the calculation, the barrel foundation was divided into 504 units. The unit type is an eight-node linear hexahedron unit with reduced integral and enhanced hourglass control. The average minimum side length of the unit is 4.17 mm, the shortest side is 0.25 mm, the average stable time increment is 4.01×10^{-7} s, and the minimum stable time increment is 2.66×10^{-7} s. The sandy soil layer around the suction foundation has a diameter and height of 700 mm and 400 mm, respectively. The calculation was not affected by the stress boundary through the infinite boundary. The sand model was divided into 10,080 units. The unit types are an eight-node linear hexahedron element and infinite eight-node linear hexahedron element with reduced integration and enhanced hourglass control. The average minimum side length is 11.2 mm, the shortest side is 5 mm, the average stable time increment is 5.14×10^{-5} s, and the minimum stable time increment is 2.45×10^{-5} s.

To conduct an effective numerical simulation, basic physical and mechanical parameters must be assigned to the model. The model used in this study was based on Chinese standard sand and steel drums (Fig. 7). To accurately describe the material properties in the model, an elastic constitutive model was used for the barrel body, and the Mohr–Coulomb

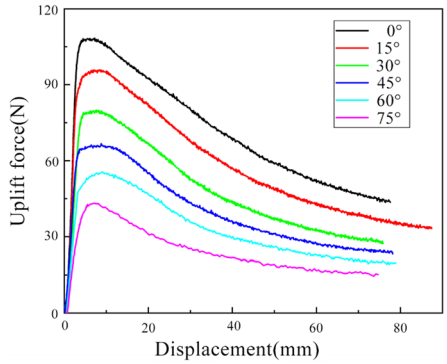

(a) 0.3 mm/s

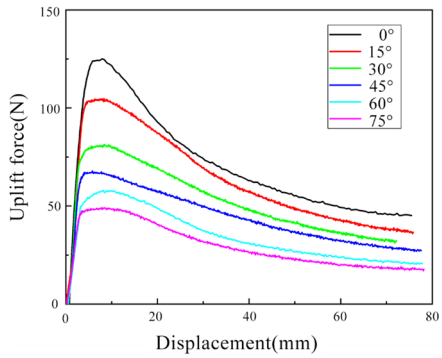

(b) 0.5 mm/s

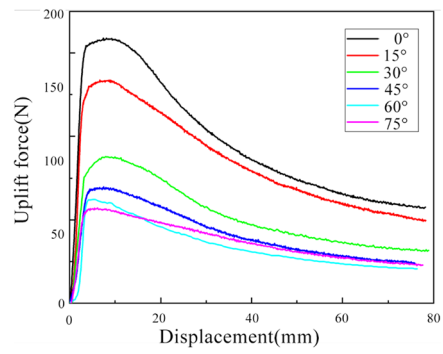

(c) 1 mm/s

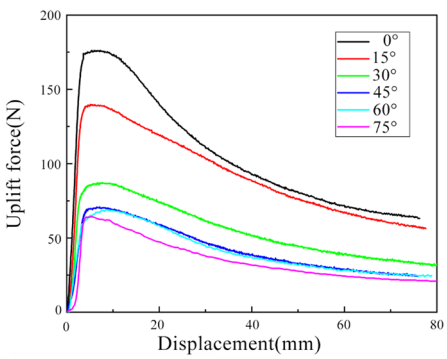

(d) 2 mm/s

Fig. 5 Bucket foundation displacement-pull-out force curves under different uplift angles

elastic–plastic constitutive model was used for the sandy soil layer. The specific model parameters are as follows: barrel density $\rho_1 = 7850$ kg/m^3, modulus of elasticity $E_1 = 210$ GPa, Poisson's ratio $\upsilon_1 = 0.125$; soil density $\rho_2 = 1580$ kg/m^3, modulus of elasticity $E_2 = 20$ MPa, Poisson's ratio $\upsilon_2 = 0.4$; soil internal friction angle of 26°, cohesion $c = 0.33$ MPa, soil undrained shear strength $S_u = 6$ kPa. The contact friction coefficient between the barrel and soil is 0.49.

3.2 Numerical Calculation and Analysis Method

A dynamic analysis of the suction bucket foundation model was conducted using ABAQUS to evaluate its dynamic characteristics when subjected to an uplift force. The dynamic analysis mainly included modal analysis and vibration shapes. Modal analysis was used to obtain the mode shapes and frequencies. This information helps in understanding the vibration characteristics of the barrel foundation under different working conditions, as well as potential resonance problems. Through the modal analysis of the mode vibration shape, the vibration shape of the suction bucket foundation model was observed. Vibration shapes can help in understanding the stress distribution and potential failure modes of a structure subjected to an uplift force.

(1) Model establishment: Three-dimensional geometric models of the barrel foundation and sand are created in ABAQUS. This involves the creation of geometry, definition of dimensions, and assembly of components.
(2) Attribute assignment: Material parameters are assigned to the barrel foundation and sand models, such as the elastic modulus, Poisson's ratio, density, friction angle, and cohesion, to accurately simulate their physical properties.
(3) Mesh division: Mesh division is performed for key parts of the model to ensure that each one has the appropriate mesh density and node correspondence. This ensures the convergence, accuracy, and efficiency of the calculation results.

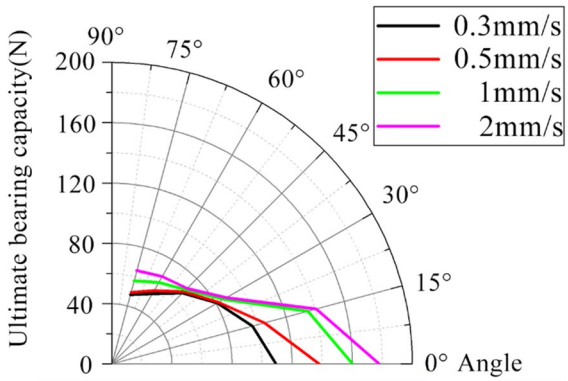

Fig. 6 Diagram of ultimate bearing capacity at different uplift speeds in the bucket foundation test

(4) Calculation of dynamic characteristics: ABAQUS is used to calculate the dynamic characteristics of the model, such as the mode shape, frequency, and vibration shape. These properties are critical for understanding the structural response to different loads.
(5) Rayleigh damping calculation: The modes of the barrel foundation and sandy soil model are analysed based on the calculated frequency. The Rayleigh damping of each model is calculated. This step is critical to accurately assess the structural response and energy dissipation capabilities under dynamic loads.
(6) Damping attribute assignment: The calculated Rayleigh damping value is assigned to the corresponding model so that the damping effect can be considered in the subsequent dynamic analysis.
(7) Component assembly: The barrel foundation and sand models are assembled to ensure that the geometric relationships and interactions between them are accurately represented.
(8) Boundary conditions and interaction property settings: Boundary conditions are added to the model, such as fixed and sliding boundaries. At the same time, the interaction properties between the barrel foundation and sandy soil, such as tangential and normal behaviours are defined, and the kinematic contact method is selected as the mechanical constraint method. Based on different drainage conditions, two interaction settings are considered. The first simulates the complete drainage situation and sets the tangential and normal stress between the barrel and soil. When the normal stress is zero, the two contact surfaces can be separated. The second simulates the partial drainage and non-drainage conditions. The sand in the bucket and the bucket itself are considered as non-separated. During the simulation process, the sand in the bucket and the bucket will move together.
(9) Load application: A gravity load is applied the model to consider the influence of the self-weight, earth pressure, and friction in the analysis.
(10) Ground stress analysis: Ground stress analysis is conducted to obtain the stress distribution inside the soil. The results of the in-situ stress analysis will be used as the initial conditions for subsequent analyses.
(11) Predefined field setting: The ground stress distribution is set as a predefined field to provide the initial conditions for the subsequent explicit dynamic analysis.
(12) Explicit dynamic analysis: An explicit dynamic analysis step is set to perform swipe displace-

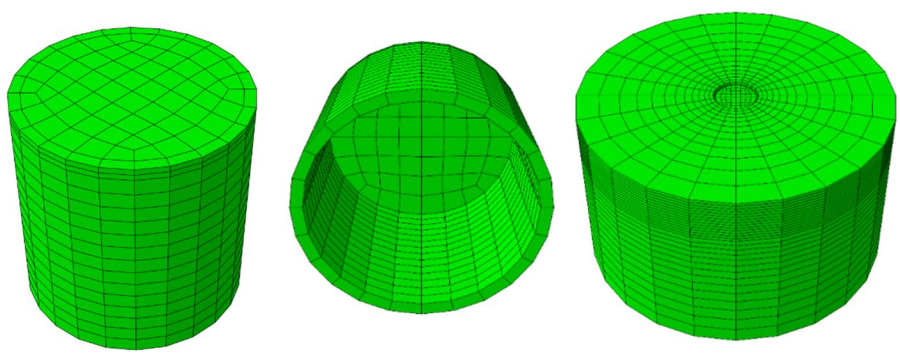

Fig. 7 Numerical model of bucket foundation

Fig. 8 Performance of ultimate bearing capacity of the tbucket foundation

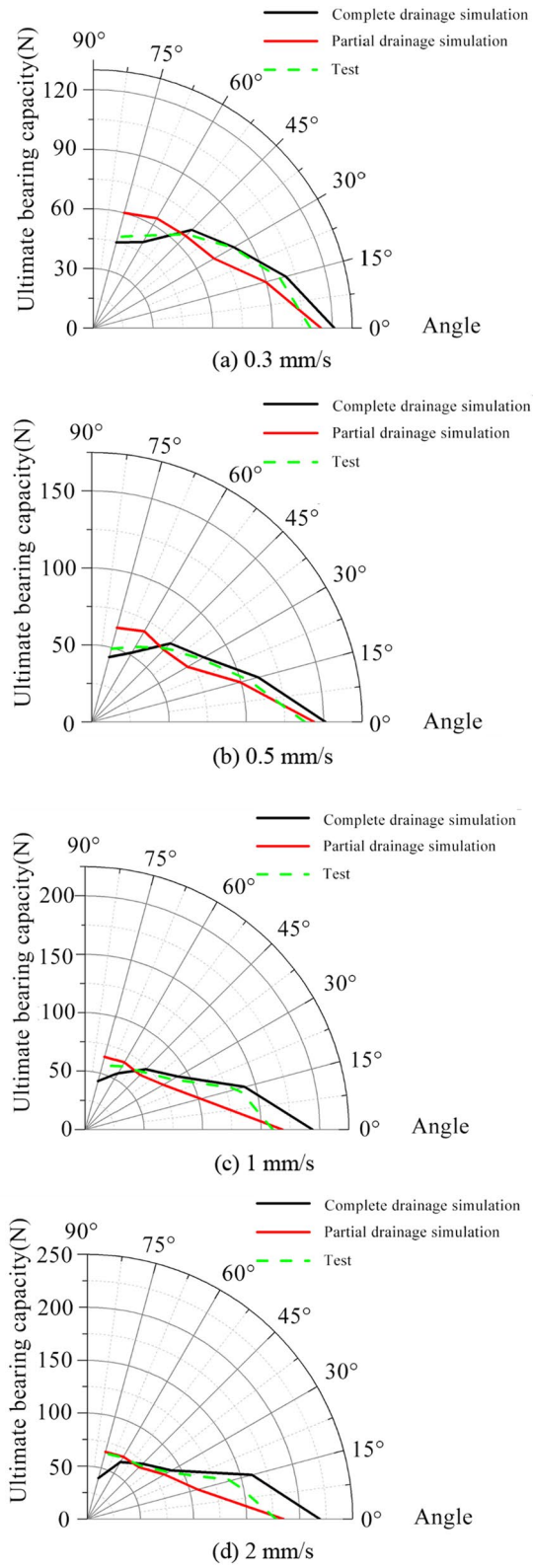

ment-controlled calculations of the dynamic loads at different angles and speeds. This will help evaluate the uplift performance of barrel foundations under different loading conditions.

3.3 Analysis of Numerical Calculation Results

Figure 8 shows the influence of different uplift angles and speeds on the uplift performance of suction foundations. (1) At the uplift speed of 0.3 mm/s, the ultimate bearing capacity of the complete drainage simulation was relatively high. The difference between the partial drainage simulation and test data was relatively small. As the uplift angle increased, the ultimate bearing capacity of the three cases showed a downward trend. At an angle of 0°, the maximum ultimate bearing capacities are 121.10 N, 114.30 N, and 109.10 N in the complete drainage simulation, partial drainage simulation, test data, respectively. At an angle of 75°, the ultimate bearing capacities are 44.72 N, 60.08 N, and 47.48 N in the complete drainage simulation, partial drainage simulation, and test data, respectively. At all angles, the ultimate bearing capacity in the fully drained simulation was generally larger, while the difference between the partially drained simulation and test data was small. (2) At the uplift speed of 0.5 mm/s, the ultimate bearing capacity in the fully drained simulation was higher, and the difference between the partially drained simulation and test data is relatively small. At an angle of 0°, the ultimate bearing capacities are 151.20 N, 143.79 N, and 137.97 N in the fully drained simulation, partial drainage simulation, and test data, respectively. At an angle of 75°, the ultimate bearing capacities are 43.57 N, 63.22 N, and 49.17 N in the complete drainage simulation, partial drainage simulation, and test data, respectively. At all angles, the ultimate bearing capacity of the fully drained simulation was generally larger, and the difference between the partially drained simulation and test data was small. (3) At the uplift speed of 1 mm/s, the ultimate bearing capacity in the fully drained simulation was relatively high,

and the difference between the partially drained simulation and test data was relatively small. At an angle of 0°, the ultimate bearing capacities are 193.87 N, 168.16 N, and 160.07 N in the fully drained simulation, partial drainage simulation, and test data, respectively. At an angle of 75°, the ultimate bearing capacities are 42.93 N, 64.25 N, and 57.11 N in the complete drainage simulation, partial drainage simulation, and test data, respectively. At all angles, the ultimate bearing capacity of the fully drained simulation was generally larger, and the difference between the partially drained simulation and test data was small. (4) At an uplift speed of 2 mm/s, the ultimate bearing capacity of the fully drained simulation was higher, and the difference between the partially drained simulation and test data was relatively small. At an angle of 0°, the ultimate bearing capacities are 218.98 N, 184.53 N, and 177.81 N in the fully drained simulation, partially drained simulation, and test data, respectively. At an angle of 75°, the ultimate bearing capacity of the complete drainage simulation is 39.99N, the partial drainage simulation is 65.52N, and the test data is 64.24N. At all angles, the ultimate bearing capacity in the fully drained simulation was generally larger, and the difference between the partially drained simulation and test data was small.

Figure 9 presents the displacement-force curves of suction caissons under various conditions. As observed in panels a to h, at penetration angles of 0°, 15°, 30°, and 45°, and at different speeds of 0.3, 0.5, 1, and 2 mm/s, the trends for fully drained simulations are similar to those of partially drained simulations. With increasing speed, there is a trend of increasing ultimate bearing capacity. However, when compared to fully drained simulations, partially drained simulations exhibit lower ultimate bearing capacities at all speeds. As indicated in panels i to l, at penetration angles of 60° and 75°, both fully drained and partially drained simulations show an opposite phenomenon at different speeds. At lower speeds, such as 0.3 mm/s, the bearing capacity curve is relatively higher, while at faster speeds, the bearing capacity decreases. Nevertheless, when compared to fully drained simulations, partially drained simulations exhibit higher ultimate bearing capacities at all speeds.

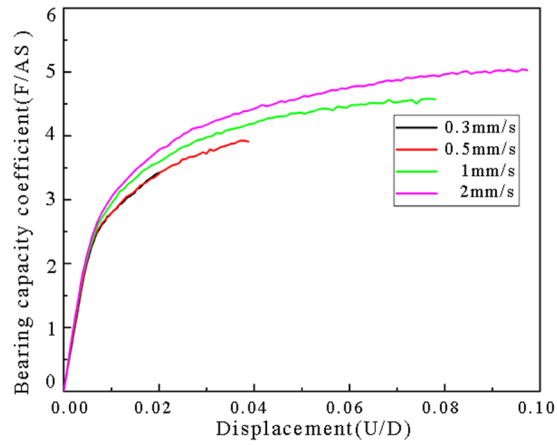

(a) 0°, Complete drainage simulation

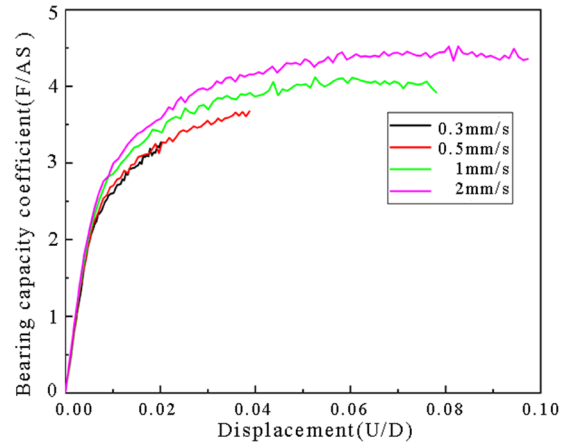

(b) 0°, Partial drainage simulation

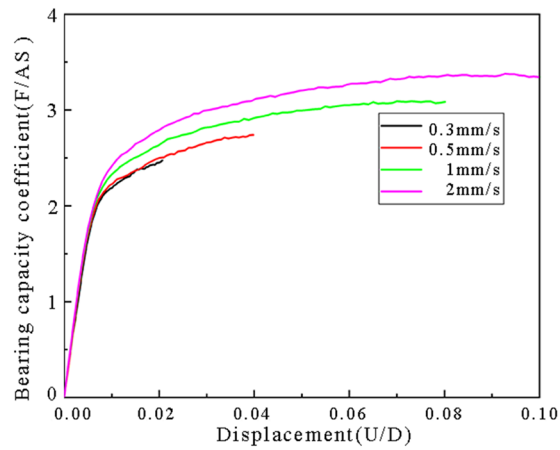

(c) 15°, Complete drainage simulation

Fig. 9 Displacement-reaction curve of bucket foundation

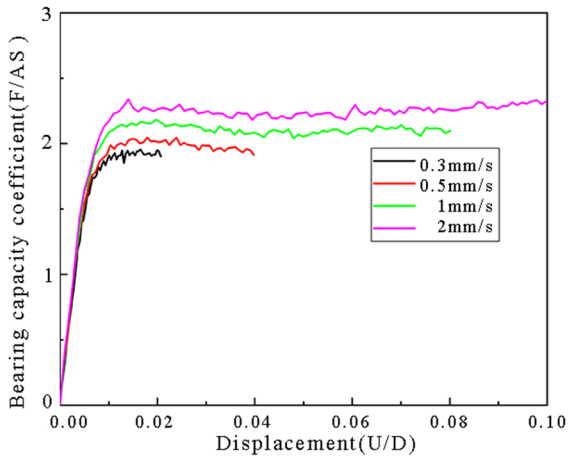

(d) 15°, Partial drainage simulation

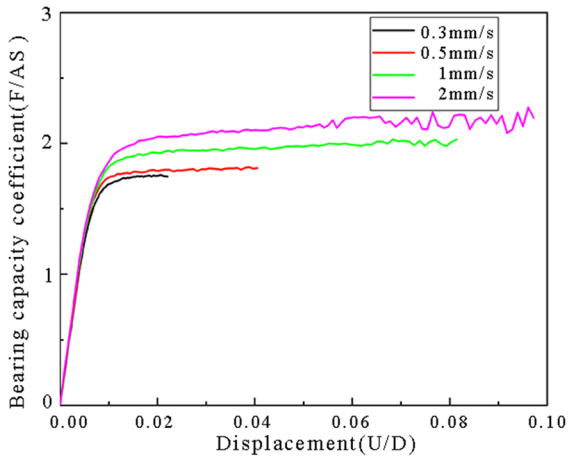

(e) 30°, Complete drainage simulation

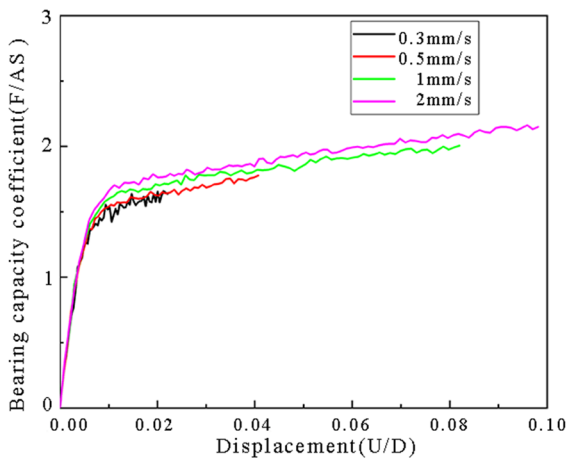

(f) 30°, Partial drainage simulation

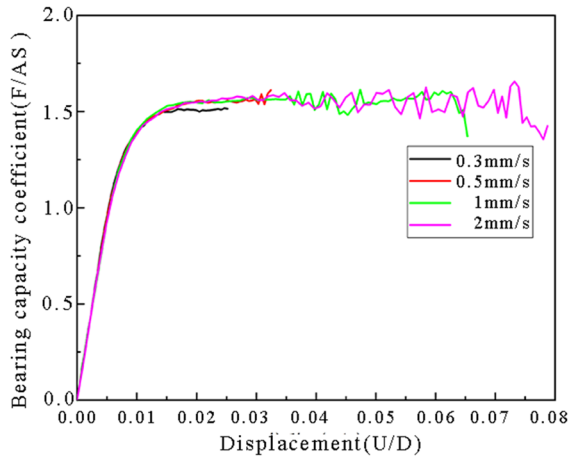

(g) 45°, Complete drainage simulation

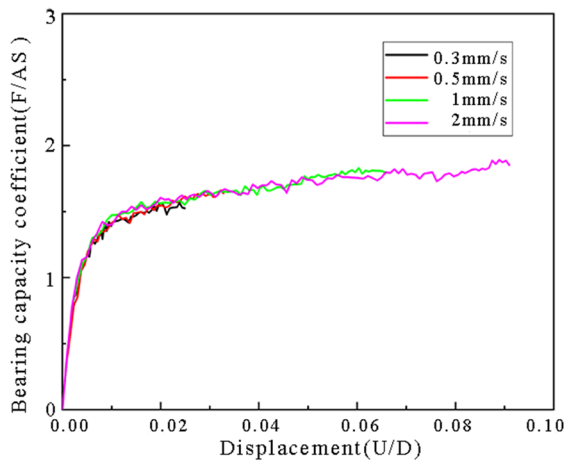

(h) 45°, Partial drainage simulation

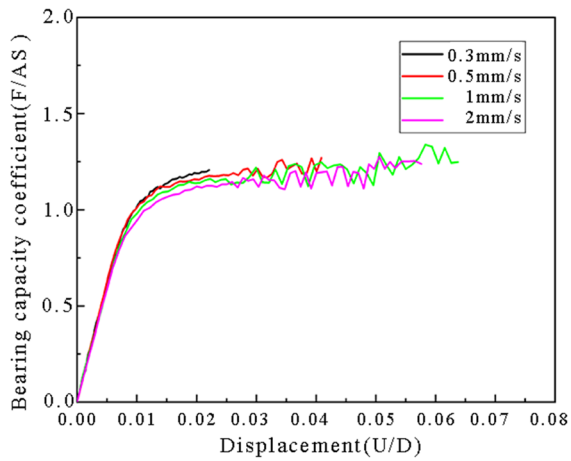

(i) 60°, Complete drainage simulation

Fig. 9 (continued)

Fig. 9 (continued)

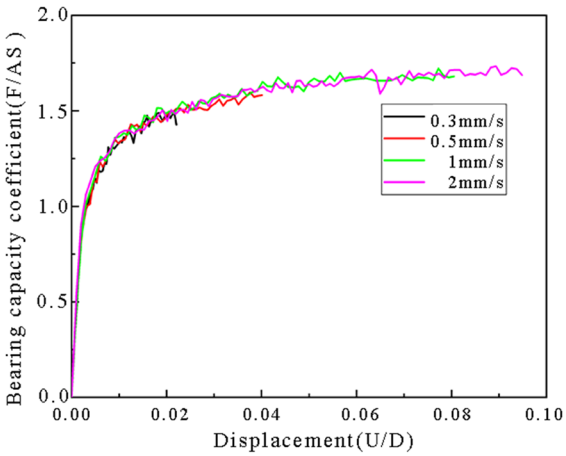

(j) 60°, Partial drainage simulation

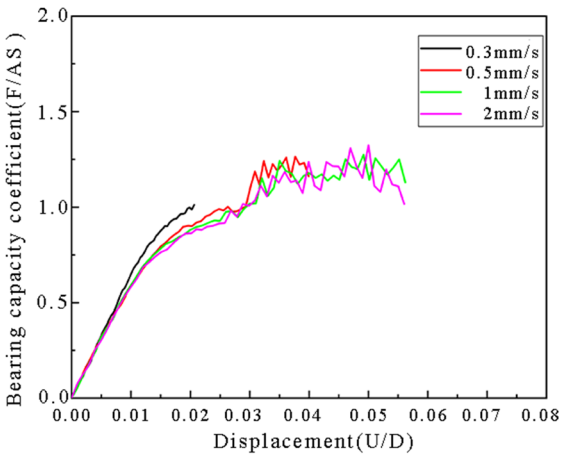

(k) 75°, Complete drainage simulation

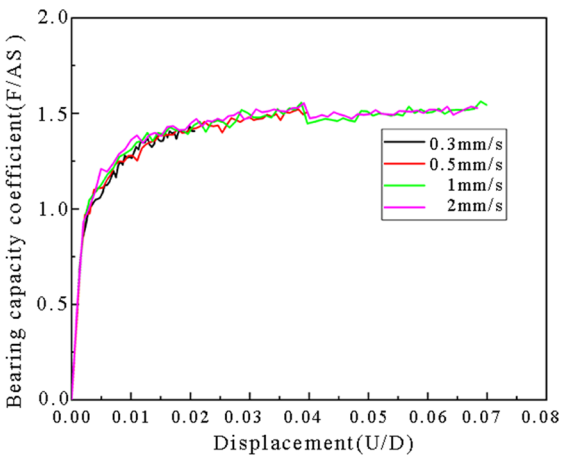

(l) 75°, Partial drainage simulation

Fig. 9 (continued)

4 Conclusion

To evaluate the uplift performance of suction foundations under different uplift angles and velocities in a saturated standard sand environment, the mechanical response characteristics of the suction foundation were compared and analysed by an indoor-scale test and numerical calculations. The conclusions of this study are as follows:

(1) At uplift angles of 0° and 15°, the change in the uplift velocity had little effect on the failure mode of the suction foundation. The main failure mode was horizontal bearing failure. At uplift angles of 30° and above, the suction foundation exhibited two damage states: circular deformation and partially drained or undrained damage.
(2) The uplift speed significantly affected the uplift performance of the suction foundation.
(3) By comparing and analysing the ultimate bearing capacities in three cases (full drainage simulation, partial drainage simulation, and test data) under the four speed conditions, it was found that the ultimate bearing capacity in the complete drainage simulation was higher overall, while the partial drainage simulation and test data were higher. The differences between the experimental data were relatively small. As the uplift angle increased, the ultimate bearing capacity in the three cases exhibited a downward trend. Fully drained simulations provide conservative safety estimates for engineering designs.
(4) Under the pull-out conditions of low uplift angles (0°, 15°, 30° and 45°), the ultimate bearing capacity of the suction foundation showed an increasing trend as the the uplift speed increased. Under the conditions of high uplift angles (60° and 75°), the simulation of the drainage state showed that the lower speed affected the uplift performance of the suction foundation.

Funding This work was supported by a grant from the National Natural Science Foundation of China (52179106).

Data Availability Enquiries about data availability should be directed to the authors.

Declarations

Conflict of interest The authors have not disclosed any competing interests.

References

Acosta-Martinez HE, Gourvenec SM, Randolph MF (2008) An experimental investigation of a shallow skirted foundation under compression and tension. Soils Found 48(2):247–254. https://doi.org/10.3208/sandf.48.247

Allersma HGB, Jacobse JA, Krabbendam RL (2003) Centrifuge tests on uplift capacity of suction caissons with active suction. The thirteenth international offshore and polar engineering conference.

Bang S, Jones KD, Kim KO et al (2011) Inclined loading capacity of suction piles in sand. Ocean Eng 38(7):915–924. https://doi.org/10.1016/j.oceaneng.2010.10.019

Cao JC (2003) Centrifuge modeling and numerical analysis of the behavior of suction caissons in clay. Memorial University of Newfoundland, Canada

Chen R, Gaudin C, Cassidy MJ (2012) Investigation of the vertical uplift capacity of deepwater mudmats in clay. Can Geotech J 49(7):853–865. https://doi.org/10.1139/t2012-037

Christensen NH, Haahr F, Rasmussen JL (1991) Breakout resistance of large suction piles.

Clukey EC, Templeton JS, Randolph MF, Phillips R (2004) Suction caisson response under sustained loop current loads. Offsh Technol Conf. https://doi.org/10.4043/16843-MS

Dai G, Zhu W, Zhai Q et al (2019) Upper bound solutions for uplift ultimate bearing capacity of suction caisson foundation. China Ocean Eng 33:685–693. https://doi.org/10.1007/s13344-019-0066-9

Deng W, Carter JP (2002) A theoretical study of the vertical uplift capacity of suction caissons. Int J Offsh Polar Eng 12:342–349

Dyvik R, Andersen KH, Hansen SB, Christophersen HP (1993) Field tests of anchors in clay–i: description. J Geotechn Eng 119(10):1515–1531

Fatolahzadeh S (2020) Experimental study of the effects of bedrock on the square skirted shallow foundations behavior. Geotech Geol Eng 38:3577–3584. https://doi.org/10.1007/s10706-020-01235-3

Fattahi H, Zandy Ilghani N (2023) Application of monte carlo markov chain and GMDH neural network for estimating the behavior of suction caissons in clay. Geotech Geol Eng 41:3305–3319. https://doi.org/10.1007/s10706-023-02455-z

Jia-Qing Du, Shou-Ji Du, Shen S-L, Ma X-F (2017) Centrifuge evaluation of influential factors in the uplift capacity of suction foundations in clay. Mar Georesour Geotechnol 35(4):456–465. https://doi.org/10.1080/1064119X.2016.1194921

Kim S, Choo YW, Kim JH et al (2015) Pullout resistance of group suction anchors in a parallel array installed in silty sand subjected to horizontal loading–Centrifuge and numerical modeling. Ocean Eng 107:85–96. https://doi.org/10.1016/j.oceaneng.2015.07.037

Lehane BM, Gaudin C, Richards DJ, Rattley MJ (2008) Rate effects on the vertical uplift capacity of footings founded in clay. Géotechnique 58(1):13–21. https://doi.org/10.1680/geot.2008.58.1.13

Liu M, Yang M, Wang H (2014) Bearing behavior of wide-shallow bucket foundation for offshore wind turbines in drained silty sand. Ocean Eng 82:169–179. https://doi.org/10.1016/j.oceaneng.2014.02.034

Morrison MJ, Clukey EC, Garnier J (1994) Behavior of suction caissons under static uplift loading. Int Conf Centr 94:823–828

Patel SK, Singh B (2019) A parametric study on the vertical pullout capacity of suction caisson foundation in cohesive soil. Innov Infrast Solut 4:1–11. https://doi.org/10.1007/s41062-018-0188-6

Purawana OA, Leung CF, Chow YK et al (2005) Influence of base suction on extraction of jack-up spudcans. Geotechnique 55(10):741–753. https://doi.org/10.1680/geot.2005.55.10.741

Qiu Y, Gao Y, Li B, Wang Y, Wu D (2017) Calculation methods for ultimate inclined bearing capacity of caisson foundation under inclined load. J Yangtze River Sci Res Inst 34(6):103–107

Rahman MS, Wang J, Deng W, Carter JP (2001) A neural network model for the uplift capacity of suction caissons. Comput Geotech 28(4):269–287. https://doi.org/10.1016/S0266-352X(00)00033-1

Rasmussen JL, Christensen NH, Haahr F (1991) Soil structure interaction model for a suction pile platform. OMAE Offsh Technol ASME 1B:601–610

Renzi R, Maggioni W, Smits F, Manes V (1991) A centrifugal study on the behavior of suction piles. Proceeding international conference on centrifuge modelling—centrifuge '91, H.-Y. Ko, ed., Balkema, Rotterdam, The Netherlands pp 169–176.

Samui P, Das S, Kim D (2011) Uplift capacity of suction caisson in clay using multivariate adaptive regression spline. Ocean Eng 38(17–18):2123–2127. https://doi.org/10.1016/j.oceaneng.2011.09.036

Senders M (2008) Suction caissons in sand as tripod foundations for offshore wind turbines, Ph.D. Thesis, University of Western Australia.

Shen K, Zhang Y, Wang K, Wang B, Zhao X (2022) Effect of partial drainage on the pullout behaviour of a suction bucket foundation, European J Environ Civil Eng 26(11):5322–5350. https://doi.org/10.1080/19648189.2021.1895891

Ssenyondo V, Hong S, Bong T et al (2021) Effects of embedment depth on the pullout capacity of bucket foundations in sand. Ocean Eng 237:109643. https://doi.org/10.1016/j.oceaneng.2021.109643

Steensen-Bach JD (1992) Recent model tests with suction piles in clay and sand. Offsh Technol Conf. https://doi.org/10.4043/6844-MS

Vaid YP, Negussey D (1988) Preparation of reconstituted sand specimens. ASTM Special Technical Publications 977:405–417. https://doi.org/10.1520/STP29090S

Vicent S, Kim SR, Bong T (2020) Effect of loading rate on the pullout capacity of offshore bucket foundations in sand. Ocean Eng 210:107427. https://doi.org/10.1016/j.oceaneng.2021.109643

Xu C, Jiang H, Xu M, Sun D, Rui S (2023) Calculation method for uplift capacity of suction caisson in sand considering different drainage conditions. Sustainability 15(1):454. https://doi.org/10.3390/su15010454

Zhao Y, Liu H, Li P (2016) An efficient approach to incorporate anchor line effects into the coupled Eulerian-Lagrangian analysis of comprehensive anchor behaviors. Appl Ocean Res 201:201–215. https://doi.org/10.1016/j.apor.2016.06.005